

# Bio-compatible miniature viscosity sensor based on optical tweezers

SHUN YUAN,<sup>1</sup> QING ZHENG,<sup>1</sup> BENJUN YAO,<sup>1</sup> MINGCONG WEN,<sup>1</sup>  
WEINA ZHANG,<sup>2</sup> JIE YUAN,<sup>3,4</sup> AND HONGXIANG LEI<sup>1,5</sup>

<sup>1</sup>*School of Materials Science and Engineering, State Key Laboratory of Optoelectronic Materials and Technologies, Sun Yat-sen University, Guangzhou 510275, China*

<sup>2</sup>*School of Information Engineering, Guangdong University of Technology, Guangdong Provincial Key Laboratory of Photonics Information Technology, Guangzhou 510006, China*

<sup>3</sup>*School of Medical Informatics, Daqing Campus, Harbin Medical University, Daqing, 163319, China*

<sup>4</sup>*yuanjie@hmdq.edu.cn*

<sup>5</sup>*leihx@mail.sysu.edu.cn*

**Abstract:** Viscosity is a fundamental biomechanical parameter related to the function and pathological status of cells and tissues. Viscosity sensing is of vital importance in early biomedical diagnosis and health monitoring. To date, there have been few methods of miniature viscosity sensing with high safety, flexible controllability, and excellent biocompatibility. Here, an indirect optical method combining the significant advantages of both optical tweezers and microflows has been presented in this paper to construct a cellular micromotor-based viscosity sensor. Optical tweezers are used to drive a yeast cell or biocompatible SiO<sub>2</sub> particle to rotate along a circular orbit and thus generate a microvortex. Another target yeast cell in the vortex center can be controllably rotated under the action of viscous stress to form a cellular micromotor. As the ambient viscosity increases, the rotation rate of the micromotor is reduced, and thus viscosity sensing is realized by measuring the relationship between the two parameters. The proposed synthetic material-free and fuel-free method is safer, more flexible, and biocompatible, which makes the cellular micromotor-based viscosity sensor a potential detector of the function and pathological status of cells and tissues in vivo without introducing any exogenous cells.

© 2022 Optica Publishing Group under the terms of the [Optica Open Access Publishing Agreement](#)

## 1. Introduction

Viscosity, is fundamental biomechanical parameter that is related to the function and pathological status of cells and tissues [1]. Intracellular viscosity also plays an important role in influencing or governing the substance exchange, signal transduction and biomolecules interactions [2,3]. Although various viscometers, such as ball viscometer and rotational viscometer, have been developed, they were just suitable for the measurement of macroscopic fluid and could not achieve the measurement at the biological cell level. Some biological or biomimetic cilium have been predicted to be as viscosity sensors, but the mechanism of drag/push force was not clear [4]. In recent years, fluorescent probes based on the principle of molecular rotors have become an important tool for measuring viscosity changes in biological systems due to their small size, simple operation, and in-situ non-destructive imaging [5]. As the viscosity increases, intramolecular rotation can be suppressed, which reduces the probability of non-radiative pathways and thus leads to an increase in fluorescence intensity [6]. So, the viscosity sensing can be realized. However, there are some problems need to be overcome in the existing probes, including sensitivity to the polarity of solvents, reactivity towards reactive oxygen species (ROS), influence of the spontaneous fluorescence of cells, and low photostability [5,7,8]. Therefore, finding a simpler and more suitable technique for use in viscosity biosensing is desirable.

Owing to the tiny size and unique mobility, the research of micromotors provides many new ideas and solutions for biomedical applications and healthcare technology. In particular,

micromotors can attach to the targets actively and enhance the mass transfer in solution, which is highly advantageous in biosensing [9]. For example, pH [10], C-reactive protein [11] and serum glucose [12] have been effectively detected using micromotors in the solution. However, viscosity biosensing based on micromotors has not been widely explored yet. Nevertheless, it was found that viscosity could affect the propulsion mechanism of micromotor, which was manifested as the change of micromotor speed [13,14]. Therefore, it is highly novel and feasible to achieve viscosity biosensing by micromotor.

Although micromotors have shown an application potential in viscosity biosensing [15], there are still some limitations to the complete application. At present, there are three currently common types of micromotors in biosensing: catalytic micromotors, magnetic micromotors and ultrasonic micromotors. Due to its powerful propulsion and extremely high locomotion speed, catalytic micromotors has been used successfully for the targeted drug delivery [16]. But, since its movement mechanism is mainly the bubble propulsion, in which the most common chemical fuel is  $H_2O_2$  [17], the cytotoxicity and catalyst life will have to be considered as it is applied to viscosity biosensing. Compared with this catalytic micromotor, the other two fuel-free micromotors driven by external fields cause less damage to organisms, making them more suitable for in vivo biosensing [18]. The magnetic and ultrasound fields have the advantages of high penetration and a strong propulsion power, which can provide a rapid and reversible control of the speed of micromotors [19–23]. However, the devices generating such external fields usually need complicated fabrication processes and/or complex set-ups. Moreover, the micromotors need additional surface modification with electrically or magnetically responsive materials [24–27]. Hence, finding a synthetic material-free micromotor with simple fabrication, tiny size, high safety, precise controllability, and biocompatibility is more significant for viscosity biosensing at the biological cell level.

Optical tweezers, as an effective tool for three-dimensional non-contact manipulation of micro-objects [28], has been used to exert an optical force on single cells to assemble living micromotors [29,30,31]. Different from the three driving mechanisms mentioned above and the other light-driven methods introducing phototropic materials [32] or using photocatalytic properties [33], the optical force can be directly exerted on the biocompatible targets and form synthetic material-free and fuel-free biological micromotors, which is safer, more flexible and biocompatible [29,30]. The feasibility of viscosity measurement by optical trap has been proved [34]. However, the optical force-based method requires the optically transparent targets materials with a refractive index difference with the surrounding environment. In our recent work, an indirect optical method combining the significant advantages of both optical tweezers and microflows has been proposed to obtain cellular micromotors with high safety, flexible controllability, and excellent biocompatibility [35]. Due to introducing the hydrodynamic force-based manipulation, the technique can be applied to a variety of biological cells without any shape and composition limited, meaning cellular micromotor can be constructed in vivo without introducing foreign cells or particles. More importantly, the hydrodynamic forces depend on fluid properties, it has a great potential for viscosity biosensing.

Inspired by the above, herein, we propose a bio-compatible miniature viscosity sensor based on optical tweezers. Optical tweezers were used to drive a single biological cell or biocompatible particle to rotate around a given circular trajectory and thus generate an microvortex within the circular trajectory. The target cell in the vortex center would be controllably rotated under the action of viscous stress and thus a cell micromotor was formed. As the ambient viscosity increases, the rotation rate of the micromotor can be changed, and viscosity sensing can be realized by measuring the relationship between the ambient viscosity and the rotation rate of the micromotor. The cellular micromotor-based viscosity sensor is more biocompatible and has the potential to detect the function and pathological status of cells and tissues in vivo without introducing any exogenous cells.

## 2. Experimental section

### 2.1. Experimental setup

The optical tweezers system consists of an Nd: YAG infrared laser (1064 nm) and an inverted microscope. The schematic diagram of the device is shown in Fig. 1. A laser beam is guided by a mirror into a computer-controlled acoustic-optic deflector for position control of optical trap and then extended by a beam expander to get a broadly collimated laser beam. After reflected by a dichroic mirror, the beam is highly focused by the water immersion objective lens and formed an optical trap in the sample chamber. The illumination light is focused on the sample through a condenser or lens for imaging. The image on the plane of the sample is collected by the objective lens and then focused into a standard charged coupled device (CCD) camera through a convex lens. Finally, the image is displayed on a computer. By changing the frequency of acoustic-optic-deflector unit, the scanning frequency (i.e. the amount of points scanned per second) of laser beam in the trapping region can be defined between 100 Hz and 100 kHz in the work. This rapid time-sharing methods allow us to create several dynamic optical traps and each of them can be further set with a trajectory by programming in MATLAB.

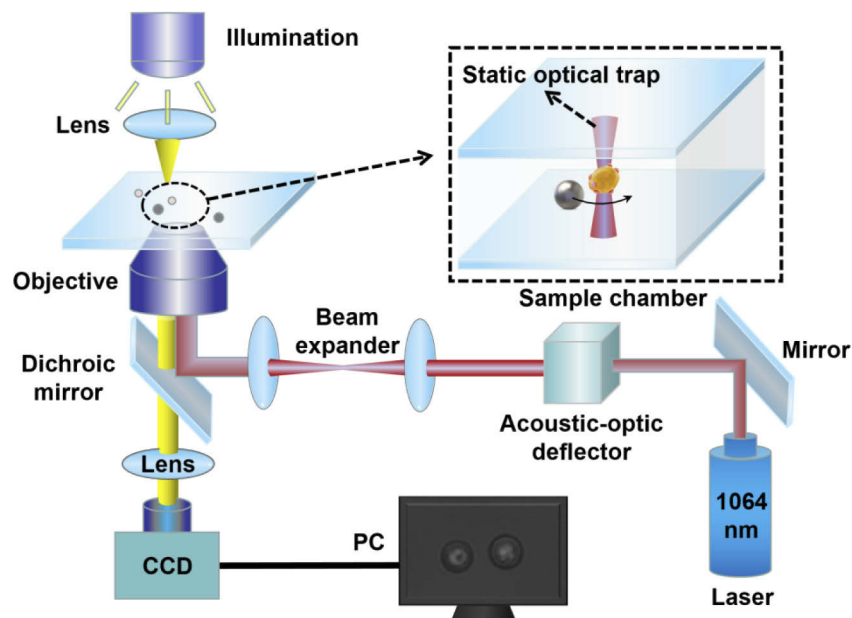


**Fig. 1.** Schematic of the experimental setup for viscosity biosensing. CCD: camera charge device.

### 2.2. Working principle of viscosity sensor and theoretical simulations

Figure 2 shows the working principle of viscosity sensor and theoretical simulations. In the theoretical model (Fig. 2(a)), a circular dynamic scanning optical trap path was set to trap and rotate an orbital particle (a single biological cell or biocompatible particle) at a constant velocity along the path. The direction and rate of its rotation can be controlled by adjusting the scanning frequency and direction of the dynamic optical trap. The relationship between the revolution rate of the orbit particle ( $R_O$ ) and the scanning frequency of the dynamic optical trap ( $f_d$ ) can be described as  $R_O = f_d / N$ . Here,  $N$  refers to the total amount of scanning points for setting the circular dynamic scanning optical trap path. In addition, it should be mentioned that, the dynamic optical trap needed to overcome Brownian motion of the orbit particle and the viscous force

exacted by the surrounding fluid. Moreover, when the viscosity increases, the viscous force acted on the orbit particle will be also increased, which need a larger laser power to maintain stable trapping. So, the laser power of the dynamic optical trap was set as the lowest value trapping the orbit particle in the suspension with a maximum viscosity ( $\sim 50$  mW in the work), which also make the orbit particle have a constant revolution rate at the different viscosity. Then the revolution of the orbit particle can make the fluid inside the circular orbit form a microvortex under the action of shear stress of fluid. The target cell in the vortex center would be controllably rotated under the action of shear stress and thus a cellular micromotor was formed. To avoid the location fluctuate of target cell, another static optical trap formed by a focused gauss light beam with a low optical power ( $\sim 3$  mW, without any optical damage) was introduced. Here, 3 mW was the lowest laser power to trap the target cell in the work. Because the magnitude of viscous shear stress is related to the viscosity of the fluid, as the viscosity changes, the force magnitude and then the rotation rate of cellular micromotor can be changed accordingly. Hence, we can measure the viscosity of the unknown fluid by measuring the rotation rate of cellular micromotor to achieve the viscosity sensing. It's worth mentioning that the temperature variation in the laser focus of the optical tweezers was estimated to be about  $1.12^\circ\text{C}$  due to the low laser power ( $3\sim 50$  mW), and thus the corresponding photothermal effects can be ignored in the experiment.

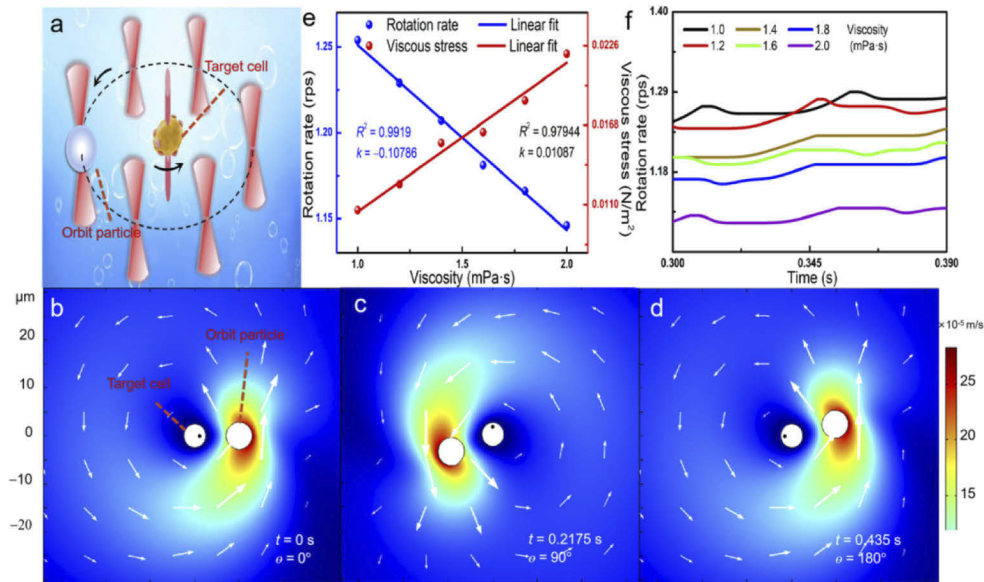


**Fig. 2.** Working principle of viscosity sensor and simulated results. a) Theoretical model. The outer red graphics represents the dynamic optical trap scanning along a circular path (black dotted line), and the center red graphic is the static optical trap for positing the target cell. b – d) The simulated distribution of fluid field around the target cell with three different rotation time at the viscosity of fluid of 2 mPa·s. The vector line of the fluid field represents the velocity field. e) The theoretical relationship between the rotation rate of the target cell and the viscosity of fluid. The corresponding viscous stress has been also calculated and plotted. f) The real-time rotation rate of target cell at different viscosity of fluid during the arbitrary two revolution periods of the orbit particle.

In order to investigate the feasibility of cellular micromotor as viscosity sensor, a series of theoretical simulations using COMSOL Multiphysics with a finite element method were performed. In the simulation, the length and width of the sample chamber was set as  $200\ \mu\text{m}$  to reduce the influence of boundary on the microflow, which was similar to the practical sample

chamber. The material of orbit particle is  $\text{SiO}_2$ , which was considered as a rigid particle. The target cell was set as an elastomer with the same parameters of yeast cell used in the experiment. The diameters of the target cell, orbital particle and circular rotation orbit were set as 5, 6 and 20  $\mu\text{m}$ . The revolution rate of the orbit particle was 2.5 rps. Density of the fluid at room temperature were set as  $1 \text{ kg/m}^3$ , which was considered as an incompressible fluid. The settings are basically consistent with the subsequent experiments. In the simulation, a real-time probe was set on the target cell surface to measure the linear speed. The average linear speed and then the average rotation rate of the cellular micromotor could be obtained from several rotation periods. As an example, Fig.2b–d shows the fluid field distribution (the viscosity of fluid: 2 mPa·s) around the target cell with three different rotation time. The dot plotted in the target cell was marked as a reference point. Obviously, a microvortex was generated when the orbit particle was rotated along a circular orbit. Thus, a cellular micromotor was formed. At this viscosity, the rotation rate of the cellular micromotor can be calculated to be 1.146 rps. To obtain the relationship between the rotation rate of the cellular micromotor and the viscosity of the fluid, more simulations have been performed, as shown in Fig. 2(e). The corresponding viscous stress has been also calculated based on Stoke's equation [35] and plotted in this figure. By increasing the viscosity from 1 to 2 mPa·s, the rotation rate of the cellular micromotor gradually decreased from 1.254 to 1.146 rps, and the viscous stress gradually increased from 0.0106 to 0.022  $\text{N/m}^2$ . Two good fitting lines of the viscosity with respect to rotation rate ( $R^2 = 0.9919$ ) and viscous stress ( $R^2 = 0.97944$ ) were achieved, where  $R^2$  refers to the fitting determination coefficient, which can represent the goodness of fit. It indicated that, the cellular micromotor can be used for viscosity biosensing. From the simulated results of fluid field with different viscosity, the real-time rotation rate of cellular micromotor was extracted for arbitrary two revolution periods of the orbit particle, as shown in Fig.2f. It shows that, during the arbitrary two periods, the cellular micromotor rotates almost smoothly, which also indicate the sensor's good stability. The above simulated results mean that the proposed method can be used to construct controllable cellular micromotor–based viscosity sensor.

### 2.3. Yeast cell micromotor-based viscosity sensor (target cell: yeast cell; orbit particle: yeast cell)

In order to realize fully biological compatibility, yeast cells ( $\sim 5 \mu\text{m}$  in diameter) were selected as both target cells and orbital particles to construct cellular micromotors. The solutions with different viscosity used in experiment were prepared by mixing glycerol and water with the mass fraction of 0%, 5%, 10%, 15%, 20%, 25%, 30%. Their viscosities were measured using constant capillary viscometer as 0.93, 1.03, 1.17, 1.39, 1.58, 1.75, 2.07 mPa·s at room temperature (23 °C), respectively. Then the dynamic optical trap was set with a scanning diameter of 18  $\mu\text{m}$ , the scanning frequency of 1000 Hz, and the laser power of 50 mW. The optical power was yet safe for the orbiting yeast cell in our experiment [35]. In this case, the revolution rate of the orbit particle was 2.5 rps. For another static optical trap for positioning the target cell, the laser power was set as 3 mW. Thus, the cellular micromotor-based sensor was constructed to measure the different viscosity at room temperature. As an example, Fig. 3(a – c) shows the rotation process of the cellular micromotor within 2 s with the viscosity of 0.93, 1.03, 1.17 mPa·s, respectively. As the viscosity increases, the rotation angle of micromotor decreases from  $450^\circ$  to  $400^\circ$  in the same time (2 s), indicating that the rotation becomes slower. In order to further analyze the relationship between the rotation rate ( $n$ ) of micromotor and the viscosity ( $\eta$ ), more experiments have been performed, as shown in Fig.3d. The data can be well fitted by the following linear equation with  $R^2 = 0.9718$ ,

$$n = -0.156 \cdot \eta + 0.754. \quad (1)$$



The slope  $k$  of this linear fitting equation is also the viscosity sensitivity, which is 0.156 rps/mPa·s. The result can help us compare with the micromotor-based sensor constructed by another orbital particle described below.

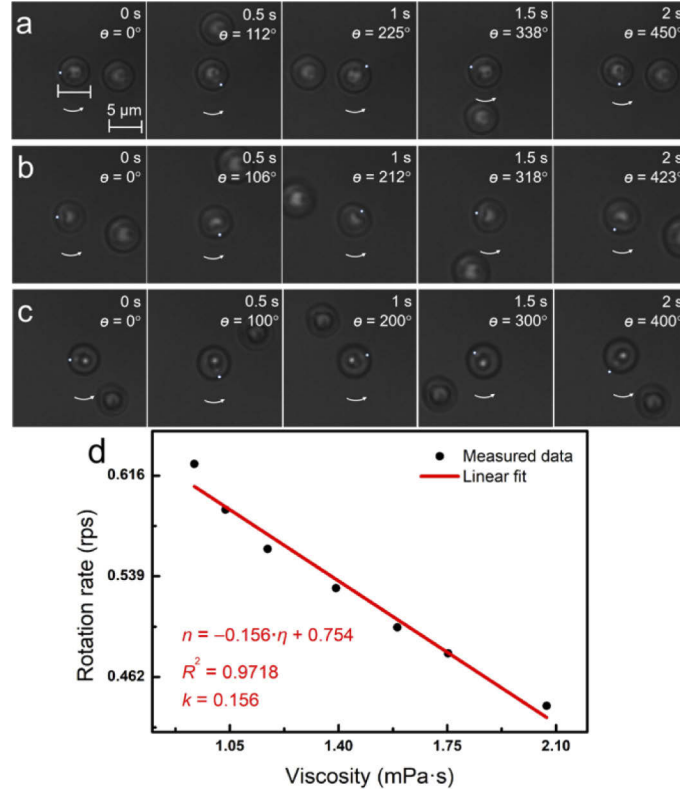


**Fig. 3.** Experimental results for yeast cell micromotor-based viscosity sensor (Target cell: Yeast cell; Orbit particle: Yeast cell). a – c) The rotation process of the cellular micromotor within 2 s with the viscosity of 0.93, 1.03, 1.17 mPa·s, respectively. d) The relationship between the rotation rate ( $n$ ) of micromotor and the viscosity ( $\eta$ ).

#### 2.4. $\text{SiO}_2$ particle/yeast cell micromotor-based viscosity sensor (target cell: yeast cell; orbit particle: $\text{SiO}_2$ particle)

Besides biological cells (yeast cells), biocompatible particles can also be as orbit particles to construct cellular micromotor-based viscosity sensor. As an example,  $\text{SiO}_2$  microspheres (diameter: 5.65  $\mu$ m) with good biocompatibility, that widely used in biomedical research, were selected as another orbit particles in our experiment while the other conditional parameters remained the same. The rotation process of the cellular micromotor within 2 s with the viscosity of 0.93, 1.03, 1.17 mPa·s was shown in Fig. 4(a – c), respectively. Similarly, as the viscosity increases, the rotation angle of micromotor decreases from 465° to 411° in the same time (2 s). Compared with the above results (5  $\mu$ m yeast cell as orbit particle), the micromotor with a larger diameter of orbit particle rotates faster, but its rotation rate yet shows a decreasing trend as the viscosity increases. By performing more experiments with different viscosity solution, the relationship between the rotation rate ( $n$ ) of micromotor and the viscosity ( $\eta$ ) was obtained, as shown in Fig.4d. The result also satisfies the linear fitting equation,

$$n = -0.159 \cdot \eta + 0.779. \quad (2)$$

The sensitivity increases to 0.159 rps/mPa·s, indicating that the diameter of the orbital particles has influence on the sensitivity of viscosity sensor. The increasing rotation rate and sensitivity were mainly attributed to the faster flow rate of microvortex that caused by the larger diameter of the orbital particles.

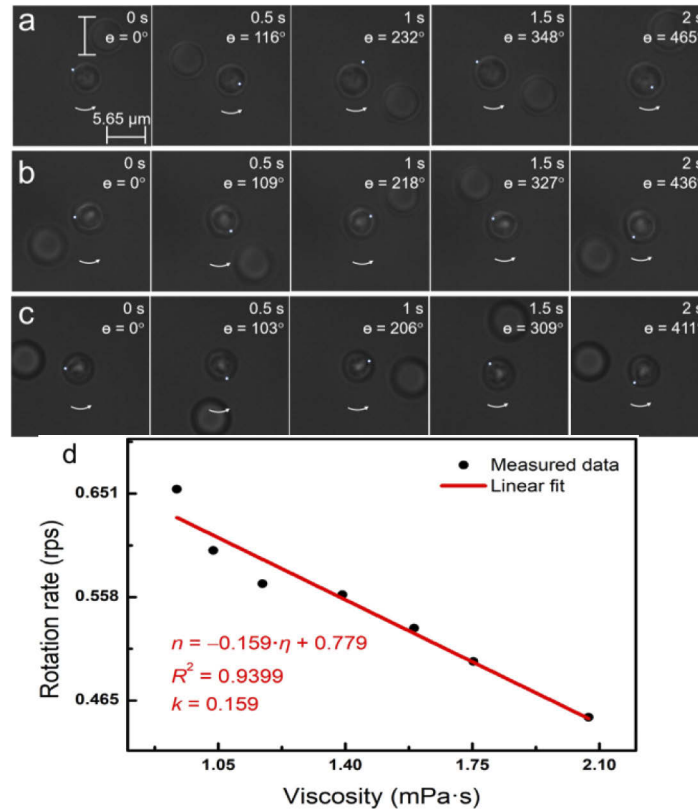


**Fig. 4.** Experimental results for SiO<sub>2</sub> particle/yeast cell micromotor-based viscosity sensor (Target cell: Yeast cell; Orbit particle: SiO<sub>2</sub> particle). a – c) The rotation process of the cellular micromotor within 2 s with the viscosity of 0.93, 1.03, 1.17 mPa·s, respectively. d) The relationship between the rotation rate ( $n$ ) of micromotor and the viscosity ( $\eta$ ).

### 3. Conclusion

Cellular micromotor-based viscosity sensors composed of biological cells (yeast cell) or biocompatible particles (SiO<sub>2</sub> particle) were constructed using optical tweezers. The method combined the significant advantages of both optical tweezers and microflows, which makes the sensor synthetic-material-free and fuel-free and have a simple fabrication, tiny size, high safety and excellent biocompatibility. It can be further used to realize viscosity sensing in vivo without introducing any exogenous cells. Besides, this method has great universality and is suitable for assembling micromotor with different materials and shapes. What's more, as the diameter of the orbit particle increases, the sensitivity of the sensor increases accordingly, which showed us an improvement direction of optimizing the sensor in future. The proposed viscosity sensor can achieve micro-area viscosity measurements at the biological cell level and will have a potential in the biomedical field, such as to measure the blood viscosity to obtain the dynamics, deformation, density and the oxygen-carrying capacity of red blood cells.

**Funding.** Natural Science Foundation of Guangdong Province (2016A030313339, 2018A030313498); National Natural Science Foundation of China (11974435, 12004444).

**Disclosures.** The authors declare no conflicts of interest.

**Data Availability.** Data underlying the results presented in this paper are not publicly available at this time but may be obtained from the authors upon reasonable request.

## References

1. F. Yang, Z. J. Chen, and D. Xing, "Single-cell photoacoustic microrheology," *IEEE Trans. Med. Imaging* **39**(6), 1791–1800 (2020).
2. X. L. E. Mu, Y. Liu, S. S. Liu, Y. L. Sun, N. N. Lu, Y. X. Lu, W. Q. Li, X. F. Zhou, B. Liu, and Z. B. Li, "A cyanine-derived near-infrared molecular rotor for ratiometric imaging of mitochondrial viscosity in cells," *Sensors and Actuators B: Chemical* **298**, 126831 (2019).
3. M. X. Hou, L. Y. Liu, K. N. Wang, X. J. Chao, R. X. Liu, and Z. W. Mao, "A molecular rotor sensor for detecting mitochondrial viscosity in apoptotic cells by two-photon fluorescence lifetime imaging," *New J. Chem.* **44**(26), 11342–11348 (2020).
4. P. R. Bandyopadhyay and J. C. Hansen, "Breakup and then makeup: a predictive model of how cilia self-regulate hardness for posture control," *Sci. Rep.* **3**(1), 1956 (2013).
5. Y. Y. Liu, Y. Y. Ma, W. J. Gao, S. H. Ma, and W. Y. Lin, "Construction of a fluorescent probe with large stokes shift and deep red emission for sensing of the viscosity in hyperglycemic mice," *Dyes Pigm.* **195**, 109674 (2021).
6. S. J. Park, B. K. Shin, H. W. Lee, J. M. Song, J. T. Je, and H. M. Kim, "Asymmetric cyanine as a far-red fluorescence probe for mitochondrial viscosity," *Dyes Pigm.* **174**, 108080 (2020).
7. G. B. Zhang, Y. Ni, D. T. Zhang, H. Li, N. X. Wang, C. M. Yu, L. Li, and W. Huang, "Rational design of NIR fluorescence probes for sensitive detection of viscosity in living cells," *Spectrochim. Acta A Mol. Biomol. Spectrosc.* **214**, 339–347 (2019).
8. L. Q. Zhu, M. L. Fu, B. Yin, L. Wang, Y. J. Chen, and Q. Zhu, "A red-emitting fluorescent probe for mitochondria-target microviscosity in living cells and blood viscosity detection in hyperglycemia mice," *Dyes Pigm.* **172**, 107859 (2020).
9. L. Kong, J. G. Guan, and M. Pumera, "Micro-and nanorobots based sensing and biosensing," *Curr Opin Electrochem* **10**, 174–182 (2018).
10. T. Patino, A. Porchetta, A. Jannasch, A. Llado, T. Stumpp, E. Schaffer, F. Ricci, and S. Sanchez, "Self-sensing enzyme-powered micromotors equipped with pH-responsive DNA nanoswitches," *Nano Lett.* **19**(6), 3440–3447 (2019).
11. A. Molinero, L. Arruza, M. A. Lopez, and A. Escarpa, "On-the-fly rapid immunoassay for neonatal sepsis diagnosis: C-reactive protein accurate determination using magnetic graphene-based micromotors," *Biosens. Bioelectron.* **158**, 112156 (2020).
12. L. Kong, N. Rohaizad, M. Z. M. Nasir, J. G. Guan, and M. Pumera, "Micromotor-assisted human serum glucose biosensing," *Anal. Chem.* **91**(9), 5660–5666 (2019).
13. A. K. Shukla, S. Bhandari, and K. K. Dey, "Dynamics of a bifunctional motor under crowded conditions," *Mater. Today Commun.* **28**, 102504 (2021).
14. P. Wrede, M. Medina, V. M. Fomin, and O. G. Schmidt, "Switching propulsion mechanisms of tubular catalytic micromotors," *Small* **17**(12), 2006449 (2021).
15. L. Shao, Z. J. Yang, D. Andren, P. Johansson, and M. Kall, "Gold nanorod rotary motors driven by resonant light scattering," *ACS Nano* **9**(12), 12542–12551 (2015).
16. D. M. Zhang, D. Wang, J. A. Li, X. Y. Xu, H. Zhang, R. M. Duan, B. Song, D. F. Zhang, and B. Dong, "One-step synthesis of PCL/Mg janus micromotor for precious metal ion sensing, removal and recycling," *J. Mater. Sci.* **54**(9), 7322–7332 (2019).
17. X. Q. Zhang, C. T. Chen, J. Wu, and H. X. Ju, "Bubble(propelled jellyfish-like micromotors for DNA sensing," *ACS Appl. Mater. Interfaces* **11**(14), 13581–13588 (2019).
18. P. L. Venugopalan, B. E. F. de Avila, M. Pal, A. Ghosh, and J. Wang, "Fantastic voyage of nanomotors into the cell," *ACS Nano* **14**(8), 9423–9439 (2020).
19. L. Liu, B. Chen, K. Liu, J. B. Gao, Y. C. Ye, Z. Wang, N. Qin, D. A. Wilson, Y. F. Tu, and F. Peng, "Wireless manipulation of magnetic/piezoelectric micromotors for precise neural stem-like cell stimulation," *Adv. Funct. Mater.* **30**(11), 1910108 (2020).
20. C. Y. Gao, Y. Wang, Z. H. Ye, Z. H. Lin, X. Ma, and Q. He, "Biomedical micro/(nanomotors: from overcoming biological barriers to in vivo imaging," *Adv. Mater.* **33**(6), 2000512 (2021).
21. T. L. Xu, L. P. Xu, and X. J. Zhang, "Ultrasound propulsion of micro-/nanomotors," *Appl. Mater. Today* **9**, 493–503 (2017).
22. C. Zhou, L. L. Zhao, M. S. Wei, and W. Wang, "Twists and turns of orbiting and spinning metallic microparticles powered by megahertz ultrasound," *ACS Nano* **11**(12), 12668–12676 (2017).
23. L. Q. Ren, W. Wang, and T. E. Mallouk, "Two forces are better than one: combining chemical and acoustic propulsion for enhanced micromotor functionality," *Acc. Chem. Res.* **51**(9), 1948–1956 (2018).



24. X. Xu, Z. Y. Huo, J. M. Guo, H. Liu, X. L. Qi, and Z. H. Wu, "Micromotor(derived composites for biomedicine delivery and other related purposes," *Bio-des. Manuf.* **3**(2), 133–147 (2020).
25. F. Y. Zhang, R. Mundaca, H. Gong, B. E. F. de Avila, M. Beltran, E. Karshalev, A. Nourhani, Y. Tong, B. Nguyen, and M. Gallot, "A macrophage–magnesium hybrid biomotor: fabrication and characterization," *Adv. Mater.* **31**(27), 1901828 (2019).
26. L. L. Wang, M. Borrelli, and J. Simmchen, "Self-asymmetric yolk-shell photocatalytic ZnO micromotors," *Chem. Photo. Chem* **5**(10), 933–939 (2021).
27. D. L. Wang, X. X. Han, B. Dong, and F. Shi, "Stimuli responsiveness, propulsion and application of the stimuli-responsive polymer based micromotor," *Appl. Mater. Today* **25**, 101250 (2021).
28. Y. J. Yang, Y. X. Ren, M. Z. Chen, Y. Arita, and C. Rosales, "Optical trapping with structured light: a review," *Adv. Photonics* **3**(3), 034001 (2021).
29. T. Pan, Y. Shi, N. Zhao, J. Y. Xiong, Y. Q. Xiao, H. B. Xin, and B. J. Li, "Bio-micromotor tweezers for noninvasive bio-cargo delivery and precise therapy," *Adv. Funct. Mater.*, 2111038 (2021).
30. H. B. Xin, N. Zhao, Y. N. Wang, X. T. Zhao, T. Pan, Y. Shi, and B. J. Li, "Optically controlled living micromotors for the manipulation and disruption of biological targets," *Nano Lett.* **20**(10), 7177–7185 (2020).
31. H. B. Xin, Y. C. Li, Y. C. Liu, Y. Zhang, Y. F. Xiao, and B. J. Li, "Optical forces: from fundamental to biological applications," *Adv. Mater.* **32**(37), 2001994 (2020).
32. D. M. Zhang, Y. Y. Sun, M. T. Li, H. Zhang, B. Song, and B. Dong, "A phototactic liquid micromotor," *J. Mater. Chem. C* **6**(45), 12234–12239 (2018).
33. R. F. Dong, Y. P. Cai, Y. R. Yang, W. Gao, and B. Y. Ren, "Photocatalytic micro/nanomotors: from construction to applications," *Acc. Chem. Res.* **51**(9), 1940–1947 (2018).
34. Q. K. Liu, T. Asavei, T. Lee, H. Rubinsztein, S. L. He, and I. I. Smalyukh, "Measurement of viscosity of lyotropic liquid crystals by means of rotating laser-trapped microparticles," *Opt. Express* **19**(25), 25134–25143 (2011).
35. X. B. Zou, Q. Zheng, D. Wu, and H. X. Lei, "Controllable cellular micromotors based on optical tweezers," *Adv. Funct. Mater.* **30**(27), 2002081 (2020).